Available online at www.sciencedirect.com
ScienceDirect
Scripta Materialia xxx (2014) xxx–xxx
Scripta MATERIALIA
www.elsevier.com/locate/scriptamat

Improved resistance to hydrogen embrittlement in a high-strength steel by quenching–partitioning–tempering treatment

Q1 Xu Zhu,[a,b] Wei Li,[b,*] T.Y. Hsu,[b] Shu Zhou,[c] Li Wang[c] and Xuejun Jin[a,*]

[a]*State Key Lab of Metal Matrix Composites, School of Materials Science and Engineering, Shanghai Jiao Tong University, Shanghai 200240, People's Republic of China*

[b]*Institute of Advanced Steels and Materials, School of Materials Science and Engineering, Shanghai Jiao Tong University, Shanghai 200240, People's Republic of China*

[c]*State Key Lab of Development and Application Technology of Automotive Steels, Baosteel Research Institute, Shanghai 201900, People's Republic of China*

Received 3 September 2014; revised 21 October 2014; accepted 23 October 2014

The effect of ε-carbide on hydrogen embrittlement (HE) susceptibility was evaluated in a quenching–partitioning–tempering (Q-P-T) treated steel. Total elongation loss (1 min hydrogen charging) drops from 42.7% to 0.6% after the tempering treatment. A significant improvement to HE is associated with the trapping capacity of ε-carbide, which is revealed by thermal desorption spectroscopy analysis and three-dimensional atom probe. A possible mechanism is discussed to explain the improved resistance to HE.

Keywords: Quenching–partitioning–tempering (Q-P-T); Hydrogen embrittlement; ε-Carbide; Hydrogen trapping; Three-dimensional atom probe (3DAP)

It is a long-standing challenge to extend the usage of advanced high-strength steels in hydrogen-rich environments, given that these steels are prone to hydrogen embrittlement (HE), by increasing their mechanical strength [1–3]. One promising way to solve this issue is the exploitation of carbides [4,5]. Carbides increase the strength by a precipitation strengthening mechanism [6,7] and simultaneously introduce strong trapping sites that immobilize hydrogen [8,9]. Successful attempts have been made in respect of the dispersion of fine cementite [10] and alloy carbides, such as titanium carbide (TiC) [4,11,12] and vanadium carbide (V_4C_3) [5,13–16].

In quenching and partitioning (Q&P) treated steel, it is possible to precipitate ε-carbide in martensite by low-temperature tempering while the precipitation of cementite is inhibited [17,18]. Transition ε-carbide is commonly recognized as ε-$Fe_{2.4}C$ with a theoretical carbon content of ~29.4 at.% [19,20]. With ε-carbide precipitating in martensite, the diffusive hydrogen amount is expected to be decreased in the vicinity of martensite–austenite interfaces, reducing the possibility of initiating hydrogen-induced cracking. In spite of extensive research on alloy carbides, no investigation has been reported on the hydrogen-trapping capacity of ε-carbide. Therefore, it is of great interest to evaluate the hydrogen-trapping capacity of ε-carbide precipitation in this steel.

Three-dimensional atom probe (3DAP) has proved to be suitable for hydrogen visualization in steel due to its high spatial resolution [8,21]. Residual hydrogen gas in the analysis chamber is inevitable and physisorbed/chemisorbed hydrogen may affect the measured hydrogen in 3DAP [8,22]. However, some researchers [23–25] have argued that in ultrahigh vacuum systems below 100 K residual hydrogen is not significant in terms of hydrogen detection. The present study additionally aims at revealing the hydrogen-trapping capacity of ε-carbide by 3DAP.

The chemical composition of the investigated steel is Fe–0.22C–1.40Si–1.80Mn (wt.%). Cold-rolled sheets (1.6 mm thick) were prepared by a Q&P process [26]. The as-received steel was then tempered at 200 °C for 2 h to precipitate sufficient ε-carbide (named quenching–partitioning–tempering (Q-P-T) steel hereinafter). Transmission electron microscopy (TEM) characterization was carried out on a JEOL 2010F.

Tensile test specimens were prepared according to ASTM Standard E 8M-04 with the long axes parallel to

* Corresponding authors. Tel./fax: +86 21 54745567 (W. Li). Tel.: +86 21 54745560; fax: +86 21 34203098 (X. Jin); e-mail addresses: weilee@sjtu.edu.cn; jin@sjtu.edu.cn

http://dx.doi.org/10.1016/j.scriptamat.2014.10.030
1359-6462/

the rolling direction [3]. Hydrogen was electrochemically charged into the specimens in an aqueous solution of 0.5 M H_2SO_4 containing 1 g l^{-1} thiourea at a current density of 30 mA cm^{-2} for 1 and 5 min at room temperature. Slow strain-rate tensile tests were conducted at a constant strain rate of 10^{-5} s^{-1} at 298 K using a Zwick universal testing machine. Thermal desorption spectroscopy (TDS) with quadrupole mass spectrometer was performed to measure hydrogen content at a constant heating rate of 100 °C h^{-1}.

3DAP measurement was conducted using a local electrode atom probe (LEAP 3000 HR). Samples for 3DAP analysis were carefully prepared [26] and electrochemically charged for 24 h (to saturate the samples with hydrogen). Finally, the rods were electropolished to sharpen needle-shaped specimens and immediately placed in the chamber (within 1 min). Identical specimens without hydrogen charging were tested for comparison. The testing temperature is around 50 K under ultra-high vacuum (4.5×10^{-11} Torr) with a pulse fraction of 0.2 and a pulse repetition rate of 200 kHz.

The engineering stress–strain curves performed on both Q&P and Q-P-T steels under different charging conditions are given in Fig. 1a. One representative curve was selected from four tests for each condition. Tempering treatment increases the ultimate tensile strength (30 ± 8 MPa) but decreases the total elongation (from 19.5 ± 0.4 to 17.9 ± 0.2%): compare the black dashed curve with the black solid curve in Fig. 1a. It is worth mentioning that the tempering treatment reduces the loss in total elongation. Fig. 1b summarizes the measured total elongations

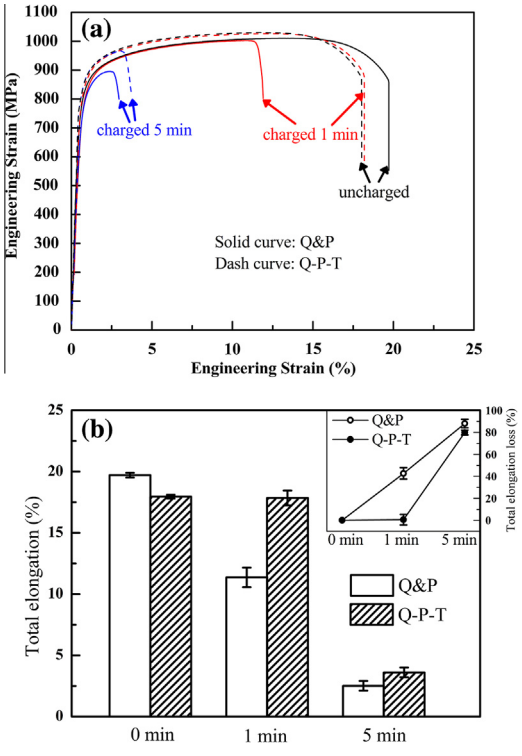

Fig. 1. (a) Engineering tensile stress–strain curves for Q&P and Q-P-T steels, cathodically hydrogen charged and immediately tested to failure at a constant strain rate of 1.0×10^{-5} s^{-1} at 298 K. (b) Total elongation of Q&P and Q-P-T steels with different hydrogen-charging conditions. The inserted graph corresponds to the calculated total elongation loss.

for each specimen. Total elongation loss (El_{loss}), which illustrates the degradation of mechanical properties, is quantified as follows:

$$El_{loss} = \frac{El_{uncharged} - El_{charged}}{El_{uncharged}} \times 100. \quad (1)$$

The value of El_{loss} increases with the prolonged charging time for both Q&P and Q-P-T steels, while the increase of El_{loss} in the Q-P-T steel is much smaller than that in Q&P steel, indicating that the tempering treatment mitigates the effect of hydrogen on the deterioration in mechanical properties.

The representative microstructure for both Q&P and Q-P-T steels consist of ferrite, martensite and retained austenite (see Supplementary Fig. S1). A bright-field image of the Q&P steel in Fig. 2a displays a typical lath-type martensite structure with a thickness of ~200–300 nm. Retained austenite is present at the interlath boundaries as shown by the dark-field image in Fig. 2b. The Q-P-T steel exhibits similar microstructures to that of the Q&P steel with the exception of needle-shaped carbides within the plate martensite (Fig. 2c and d). These are confirmed as ε-carbides based on the inserted selected-area electron diffraction (SAED) analysis.

Typical TDS curves of Q&P and Q-P-T steels under the same charging conditions are shown in Fig. 3. Hydrogen charging induces a pronounced desorption peak at ~90 °C, which is suggested to be the result of reversible trapping sites (diffusible hydrogen) due to the combination of grain boundaries, retained austenite and dislocations [4,27,28]. The TDS peak at ~400 °C is usually considered to be the result of irreversible trapping sites (such as carbides) due to the strong trapping effect [29,30]. A key finding is that the nondiffusible hydrogen content in Q-P-T is higher than that in Q&P steel, while the diffusible hydrogen content is lower. Since only ε-carbides are precipitated during tempering treatment, it is thus reasonable to deduce that the nondiffusible hydrogen in our work is correlated to ε-carbides.

Fig. 4 illustrates the 3DAP result of hydrogen uncharged and charged Q-P-T steel, showing the distribution of carbon atoms (red) and hydrogen atoms (green). The carbon agglomeration regions in Fig. 4c, e and h correspond to ε-carbides based on their size and morphology. In the absence of hydrogen charging, little hydrogen is detected in the matrix (Fig. 4b). Even around the ε-carbide, a small amount of hydrogen is observed (Fig. 4d). By contrast (Fig. 4d and g), most hydrogen atoms are introduced by electrochemical charging (24 h) prior to the 3DAP sample preparation. Hydrogen atoms in the hydrogenated specimen tend to be trapped at ε-carbides (Fig. 4g and i).

The results indicate that low-temperature tempering of the Q&P steel enhances resistance to hydrogen degradation. During the tempering process at low temperature, other phase transitions and microstructure evolutions should be considered, such as decomposition of retained austenite and decrease in the dislocation density in martensite [17,19]. The volume fraction of retained austenite based on magnetization measurement in Q&P and Q-P-T steel is 9.01% and 9.08%, respectively (see Supplementary Fig. S2). Moreover, the variation in dislocation density is negligible for Q&P and Q-P-T steels based on a comparison of their Snoek–Köster (SK) peaks using internal friction spectra (see Supplementary Fig. S3). Therefore, the